Electrotonic Effect on Action Potential Dispersion with Cellular Automata

Ricardo Silva Campos[1,2(✉)], João Gabriel Rocha Silva[1,3], Helio José Corrêa Barbosa[1,2], and Rodrigo Weber dos Santos[1]

[1] Federal University of Juiz de Fora, Juiz de Fora, Brazil
ricardo@ice.ufjf.br, rodrigo.weber@ufjf.edu.br
[2] Laboratório Nacional de Computação Científica, Petrópolis, Brazil
hcbm@lncc.br
[3] Federal Institute of Education, Science and Technology of Mato Grosso, Pontes e Lacerda, Brazil
joao.silva@plc.ifmt.edu.br

Abstract. In this study we used a simplified electrophysiological simulator of the heart, based on cellular automata, for studying the electrotonic effect. This effect is caused by interaction between cells which changes their behavior. This feature homogenizes the repolarization dispersion, that leads all cells to return to their resting potential at the same time, regardless of their initial action potential duration, in order to avoid undesired excitation.

For achieving this feature on our automata, we proposed a new method for updating the action potential duration, by evaluating the current duration, propagation velocity and tissue conductance. The results suggest that, despite its simplicity, our simulator is suitable to mimic traditional models based on differential equations.

Keywords: Cardiac simulation · Cellular automata · Repolarization dispersion · Electrotonic effect

1 Introduction

Heart diseases are associated with high mortality rates worldwide. The development of medicines, medical devices, and non-invasive techniques for the heart demand multidisciplinary efforts towards the characterization of cardiac function.

In particular, the important phenomenon of electric propagation in the heart involves complex non-linear biophysical processes and structures. Its multi-scale nature spans from genes and nanometre processes, such as ionic movement and protein dynamic conformation, to centimetre phenomena such as whole heart

This work was supported by the National Council for Scientific and Technological Development (CNPq) - Brazil (grants 153465/2018-2 and 312337/2017-5).

© Springer Nature Switzerland AG 2020
O. Gervasi et al. (Eds.): ICCSA 2020, LNCS 12249, pp. 205–215, 2020.
https://doi.org/10.1007/978-3-030-58799-4_15

structure and contraction. The electrical activation triggers the tissue deformation that ejects blood from the ventricles. Abnormal changes in the electrical properties of cardiac cells and in the tissue structure can lead to life-threatening arrhythmia and fibrillation. Cardiac modelling challenges science in many aspects. The multi-scale and multi-physics nature of the heart bring new challenges to the mathematical modelling community, since sophisticated techniques are necessary to cope with them. In addition, a complete whole organ model would have to include all the physics and their interactions. Whereas a lot of research work has been done in the formulation of electrical models, structural-mechanics or fluid-mechanics, mathematical formulations that include all the interactions of the aforementioned physics are still incipient. As a multidisciplinary research field, a background on biology, biophysics, mathematics, and computing is necessary during the development and use of cardiac models. In particular, the implementation of the mathematical models is a time consuming process that requires advanced numerical methods and computer programming skills. In addition, the numerical resolution typically demands high performance computing environments, in the case of large simulations (tissue or organ-level models), and parallel programming expertise may add more complexity to this multidisciplinary area of research.

In general, the cardiac activity is described by non-linear systems of differential equations with tens of variables and close to a hundred parameters. Cardiac cells are connected to each other by gap junctions creating a channel between neighbouring cells and allowing the flux of electrical current in the form of ions. An electrically stimulated cell transmits an electrical signal to the neighbouring cells allowing the propagation of an electrical wave to the whole heart which triggers contraction. An electrical signal is propagated from one cardiac cell to its neighbors, in a process that triggers the mechanical contraction. This phenomenon is usually modelled using partial differential equations (PDEs) [17].

Although the PDEs used for cardiac modelling are able to perform realistic tissue simulations, they involve the simulation of thousands of cells, which make their numerical solution quite challenging. This is an issue for clinical software that may demand accurate results in real-time simulations. Therefore, some effort has been made in speeding up the PDE solvers via parallel computing [14], as well as by different techniques to emulate PDEs simulations with less computational cost [1].

In a previous work [4] we proposed a simple and fast discrete simulator, named FisioPacer. It is a 3D electro-mechanical model of cardiac tissue, described by the coupling of a cellular automata (CA) and mass-spring systems (MSS). It was able to mimic the action potential propagation and tissue contraction obtained by PDE solvers in less computational time. In this work, we propose a modification on the cellular automata, in order to add realism to our model, by changing the action potential features according to mechanical coupling of cells, the so called electrotonic effect [2]. Some features of the tissue are evaluated, such as the different action potential morphology, velocity of propagation and conductance, and then a new action potential duration (APD) is

automatically set to each cell. Preliminary results suggest our model is able to mimic experimental results of electrotonic effect from traditional models based on PDEs, easily found on literature [6,10,11].

1.1 Related Studies on Electrotonic Coupling

The heart tissue is composed of three layers: epicardium, myocardium, and endocardium. Epicardium is the outer layer and its function is to protect the inner parts. Myocardium is the middle and thickest layer. It is composed of muscle fibers, which are responsible for the heart contraction. Endocardium is the inner layer of the heart. It is thin and covers the heart chambers. The electric pulse starts at the endocardium and flows to the epicardium. The cells in each layer have different physiological properties, in particular, they have different action potential duration (APD). In normal conditions, the mid-myocardium (M-cells) have a longer AP than endo and epicardium cells. This difference is noticed in isolated cells. However, when the three types of cells are arranged together, they are connected by gap junctions. The level of coupling between neighboring cells during deformation can change their physiological properties; that's called the electrotonic effect. It changes the action potential duration [13] and the repolarization dispersion [15,16]. Thus, the change on APD homogenizes the repolarization dispersion. This means cells can be excited in different times, but their AP tend to return to resting potential at the same time, despite the difference in their APD and the distance among cells. This mechanism avoids undesired excitation caused by late repolarized cells.

As a matter of comparison, we used the Luo and Rudy model (LRd) [9], which is built based on experimental data. Its ionic currents reproduce the action potential of mammalians, mostly guinea pigs. Later, the work of Viswanathan *et al.* [18] proposed a set of experiments with LRd model for observing the impacts of the electrotonic effect. It shows how the flow of electric current changes the action potential on membrane of coupled cells, aiming at evaluating the importance of some ionic currents in the heterogeneity of repolarization.

For instance, in guinea pigs, the APD of isolated epicardial cells, endocardial cells, and M cells are 160, 185, and 250 ms, respectively [18], which means the APD difference between midmyocardium and epicardial cells (ΔAPD) is 90 ms. On the other hand, M, epi and endocardium cells combined resulted in $\Delta APD = 18$ ms. The coupling of cells is determined by conductance of gap junctions and by AP propagation velocity [12]. Therefore, decreasing the cell coupling level increases the ΔAPD.

2 Methods

A cellular automaton is a model of a spatially distributed process that can be used to simulate various real-world processes. A two-dimensional cellular automaton consists of a two-dimensional lattice of cells where all cells are

updated synchronously for each discrete time step. The cells are updated according to some updating rules that will depend on the local neighborhood of a particular cell.

The idea of macroscopically simulating the excitation-propagation in the cardiac tissue with a CA was proposed in [8] and extensively used in the literature [3,7]. The CA is built on the idea that a single cell gets excited if the electrical potential exceeds a determined threshold. Once it is excited, it can trigger the excitation of neighboring cells. In this manner, an electrical stimulus will propagate through the CA grid as the time steps are computed. In this work, the CA states are related to the action potential (AP) and force development in a cell. To make CAs more efficient they are usually parameterized using simulated data from accurate models. This means that the states related to the AP in the cell will be related to a specific portion of the cardiac cell potential. Figure 1 Part A presents the AP computed by ODEs, the AP divided into five different states that represent the different physiological stages of the AP.

In state S0 the cell is in its resting potential where it can be stimulated, in S1 the cell was stimulated and can stimulate the neighbors. In S2 the cell is still able to stimulate the neighbors. In S3 the cell is in its absolute-refractory state where it cannot be stimulated and does not stimulate its neighbors. In S4 the cell is in its relative refractory state where it can be stimulated by more than one neighbor but it does not stimulate its neighbors. As described, the states of a cell generate rules for when a cell can stimulate a neighbor and when it can be stimulated. These rules are an important aspect which will allow the stimulus to propagate.

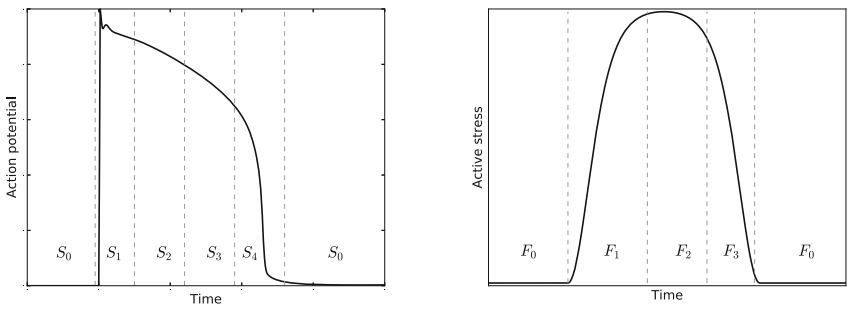

(a) Action potential states. (b) Active force states.

Fig. 1. Action potential and active force of a cardiac cell computed by ordinary differential equations and their respective representation via CA.

Another important point is how the cells change their states. The AP has a predetermined period so that the states will be spontaneously changed after the AP starts, where the time of each state is a parameter of the system. Our CA is adapted to work with irregular meshes of tetrahedrons. In that case, the cells

of the system are the tetrahedrons and a cell is considered a neighbor of other cell if they share at least one vertex. The distance between two neighbors cells is computed as the distance between their barycenters, given by:

$$\boldsymbol{X}_b^i = \frac{1}{4}\sum_{a=1}^{4} \boldsymbol{x}_a^i, \tag{1}$$

where x_a are the coordinates of the vertices from tetrahedron x^i.

Equally important, CA states are updated at every discretized time, dt. Based on the distance, velocity (passed as parameter to the model) and activation time it is possible to calculate the time that a stimulus takes to travel from one CA cell to another, in order to propagate the action potential. An anisotropic tissue was used, so that the propagation velocity is different in the three directions of interest in the heart tissue: fiber, sheet, and normal-sheet. To find the time t for a stimulus to travel from one cell to another, first the direction between the barycenters is computed and then the distance d:

$$\boldsymbol{D}_{ij} = \boldsymbol{X}_b^j - \boldsymbol{X}_b^i \tag{2}$$

$$d = \|\boldsymbol{D}_{ij}\|, \tag{3}$$

where $\boldsymbol{X}_b^i$ and $\boldsymbol{X}_b^j$ are the positions of the barycenter of elements i and its neighbor j. Next, the total velocity of the AP is calculated, based on the velocities in each one of the directions: v_f, v_s and v_n:

$$\boldsymbol{V} = v_f\boldsymbol{F} + v_s\boldsymbol{S} + v_n\boldsymbol{N}, \tag{4}$$

$$v = |\boldsymbol{V} \cdot \widehat{\boldsymbol{D}}_{ij}|, \tag{5}$$

where $\boldsymbol{F}$, $\boldsymbol{S}$ and $\boldsymbol{N}$ are respectively fiber, sheet and normal normalized directions. $\widehat{\boldsymbol{D}}_{ij}$ is the normalized direction between elements i and j. Then the traveling time t of the propagation between them is:

$$t = \frac{d}{v}, \tag{6}$$

That verifies if there is enough time to propagate the stimulus by comparing the time since the neighbor has been stimulated and time t.

Finally, electrical potential is coupled with the active force, which is responsible for starting the contraction of the cardiac tissue. When the cell is stimulated, there is an increase in the concentration of calcium ions inside the cell, which triggers the cell contraction. The force development has a delay after the cell is stimulated because of its dependence on the calcium ions. The force development of a cell can be represented in states that change over time like the electrical potential states. Figure 1 Part B presents the force development states and its relation with the electrical states. The force-development states will only pass from state F0 (no contraction force) to state F1 when the electrical state of the cell goes from state S1 to S2. After this change, force development will be time dependent, but will not depend on the electrical state of the cell.

2.1 The AP Repolarization Homogenization

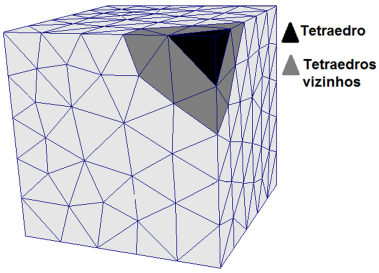

Fig. 2. A cell and its neighbors.

Our implementation changes a cell APD according to its neighbors. Every cell that shares at least one node is considered a neighbor, as is depicted in Fig. 2. So, for each cell, we first compute the average APD of all neighbors:

$$APD_t^{avg} = \sum_{i=0}^{n} APD_t^i, \tag{7}$$

where APD_t^i is the APD at time t of neighbor i. Then we compute the cell coupling level, for quantifying the degree of collaboration among cells varying on time:

$$c_t = p \times f_t \tag{8}$$

where is $p \in [0, 1]$ is parameter to represent the conductance, a user-defined value, and f_t is the normalized active force given by cellular automata in percentage values. When the force reaches its maximum value ($f = 1$), it is on its maximum deformation, so the cells are in the most coupled state, due to their contraction. Therefore, the maximum contribution of neighbors to a cell APD is reached. When that is zero, it means the cell does not accept any contribution and its APD remains unchanged. Finally, the new APD is given by:

$$APD_{t+1} = (1 - c_t) \times APD_t + c_t \times APD_t^{avg}. \tag{9}$$

3 Results

Our experiments have the setup presented in the work of Viswanathan *et al.* [18]. We simulated a tissue segment containing the same amount of the three types of cells. We stimulated cells on endocardium wall $x = 0$, and so the polarization wave flows from endo to epicardium. This configuration is shown in Fig. 3.

Viswanathan *et al.* [18] used two parameters for determining the level of coupling. The velocity of propagation v_p, given in mm/s, and gap junction conductance g_j, given in μS. They both are homogeneous in the tissue. Different



Fig. 3. Distribution of cell types in fiber.

values were tested for each simulation, to represent different levels of coupling. For a healthy tissue, it was used $(v_p, g_j) = (560, 2.5)$, typical values for simulating a normal coupling. Isolated cells represent the absence of gap-junction coupling. Intermediate configurations stand for reduced coupling, where the velocity value is typical for propagation transverse to fiber $(v_p, g_j) = (180, 0.25)$, and poorly coupled, that happens in pathological conditions such as infarction $(v_p, g_j) = (35, 0.025)$. For comparing these experiments, it was used the ΔAPD, that considers the difference of action potential duration of M-cells and epicardium cells, in the middle of respective regions. They have the corresponding maximum and minimum duration. Thus, for normal coupling, ΔAPD is 18 ms. For isolated cells, ΔAPD is 90 ms. As the level of coupling decreases, ΔAPD increases, tending to the value of isolated cells. For reduced and poor coupling, the difference on APD is respectively 44 and 72 ms.

In our FisioPacer simulations we used the same value for propagation velocity, but the gap-junction conductance g_f needed to be different, since in our model it is a percentage value, and not an absolute value of electric conductance as in the LRd model. For tuning the FisioPacer coupling, we manually tested g_f, until we obtain the same ΔAPD for the LRd model. The respective conductance g_f for poor, reduced and normal coupling is 1.64%, 4.30% and 10.5%.

Initially, the cells are set with the isolated cells APDs. During the simulation, the model applies the Eq. 9, in every time step. Therefore the APD of each cell is updated. The initial and final APD for each cell type and experiment can be found in Table 1. These values are measured in the middle of each region.

Table 1. APDs (ms) at the end of simulation, per coupling and cell-type.

Coupling	Cell type		
	Endo	Mid	Epi
Isolated	185	250	160
Poor	191	241	169
Reduced	200	223	178
Normal	206	208	190

For a better visualization, we plotted all APDs over the tissue on Fig. 4 for FisioPacer simulations. When there is no cell coupling, they remain with the same APD. Therefore we can see all cells of region with the same duration,

in the solid line in the figure. For a normal tissue, the APD over the tissue is homogeneous, so the curve of normal tissue is smoother, as there is more coupling, so ΔAPD is smaller. For reduced and poor coupling, ΔAPD is greater and therefore the curve is less flat than normal. As the level of coupling decreases, the APD curve tends to be closer to that of isolated cells. These curves are similar to those obtained by the LRd model in Viswanathan *et al.* [18].

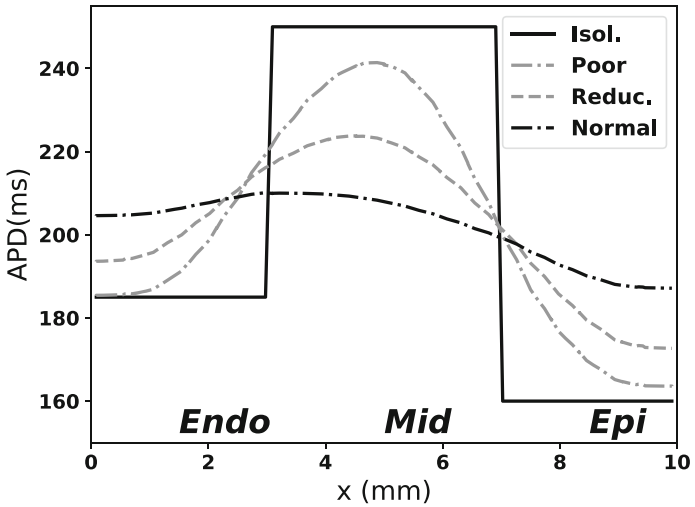

Fig. 4. Action potential duration with different coupling level, over the tissue.

The action potential for each tissue configuration can be found at Fig. 5. For isolated cells, since there is no cell coupling, the AP remains in its original duration (Fig. 5a). For poor coupling, propagation velocity is low, therefore the polarization wave takes more time to reach the epicardium cells. Besides that, the conductance is also low, so there is less interaction on cells and less changes on ΔAPD. For reduced coupling, the velocity is greater and thus the epicardium is excited sooner. The ΔAPD is lesser than poor coupling, since conductance is greater. Finally, the normal coupling results in a very fast depolarization, making cells excited in close moments. The ΔAPD is low, due the high conductance and therefore cells return to resting almost together, i.e., the repolarization dispersion is homogeneous.

The performance was very fast. We used a finite element mesh containing 518 tetrahedrons. We simulated 500 ms of cardiac tissue activity, with a timestep of 0.1 ms. In a Windows 10 desktop computer with an i7 processor and 16 gb RAM, our simulation took in average 420 ms to run.

In our previous works, we performed a comparison with another simulator based on a traditional finite element approach. FisioPacer was up to 90 times faster, depending on simulations configuration [5].

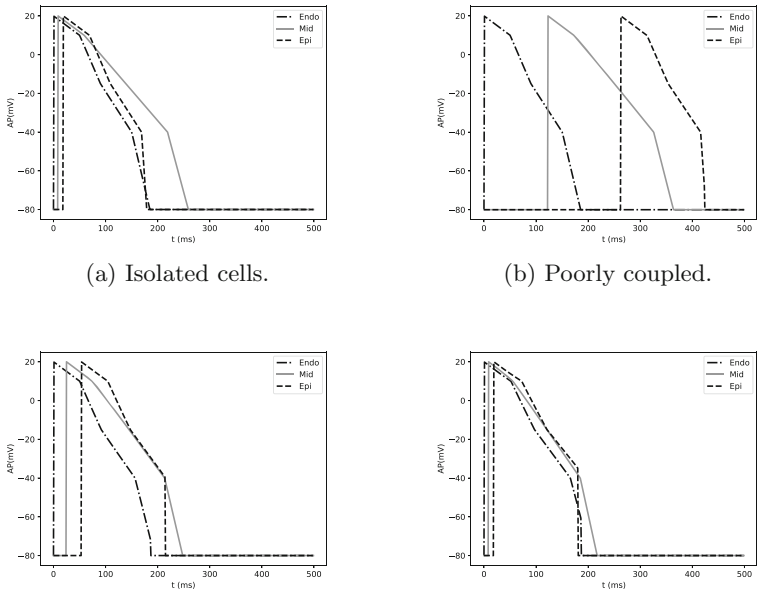

(a) Isolated cells.

(b) Poorly coupled.

(c) Reduced coupling.

(d) Normal coupling.

Fig. 5. Action potential of endo, mid and epicardium cell with different coupling levels.

4 Conclusion

In this work we presented a cardiac simulator based on cellular automata, that was modified to represent the electrotonic effect. This effect occurs due to the cell coupling, where cells interact with each other and therefore their behavior can change.

Specifically, this interaction can change the action potential duration (APD), in order to prevent undesired propagation waves. For instance, isolated cells have a very different APD. For guinea pig models the difference between mid-myocardium and epicardium is around 90ms. However, in a healthy tissue, this difference decreases 18 ms, 20% of the original value. In this sense, we adapted our model for reproducing the APD change, according to parameters found in the literature, such as tissue conductance, propagation velocity and APD of neighbor cells. Despite the simplicity of our methods, our simulator was able to reproduce results of another simulator, obtaining the same ΔAPD in different coupling levels.

References

1. Atienza, F.A., et al.: A probabilistic model of cardiac electrical activity based on a cellular automata system. Revista Española de Cardiología (English Edition) **58**(1), 41–47 (2005)
2. Bazhutina, A., Balakina-Vikulova, N., Solovyova, O., Katsnelson, L.: Mathematical model of electrotonic interaction between mechanically active cardiomyocyte and fibroblasts. In: 2019 Ural Symposium on Biomedical Engineering, Radioelectronics and Information Technology (USBEREIT), pp. 114–117. IEEE (2019)
3. Bora, C., Serinağaoğlu, Y., Tönük, E.: Electromechanical heart tissue model using cellular automaton. In: 2010 15th National Biomedical Engineering Meeting, pp. 1–4. IEEE (2010)
4. Campos, R.S., Rocha, B.M., Lobosco, M., dos Santos, R.W.: Multilevel parallelism scheme in a genetic algorithm applied to cardiac models with mass-spring systems. J. Supercomput. **73**(2), 609–623 (2017)
5. Campos, R.S., Rocha, B.M., da Silva Barra, L.P., Lobosco, M., dos Santos, R.W.: A parallel genetic algorithm to adjust a cardiac model based on cellular automaton and mass-spring systems. In: Malyshkin, V. (ed.) PaCT 2015. LNCS, vol. 9251, pp. 149–163. Springer, Cham (2015). https://doi.org/10.1007/978-3-319-21909-7_15
6. Dos Santos, R.W., Otaviano Campos, F., Neumann Ciuffo, L., Nygren, A., Giles, W., Koch, H.: ATX-II effects on the apparent location of M cells in a computational model of a human left ventricular wedge. J. Cardiovasc. Electrophysiol. **17**(s1), S86–S95 (2006)
7. Gharpure, P.B., Johnson, C.R., Harrison, N.: A cellular automaton model of electrical activation in canine ventricles: a validation study. SCI Institute (1995)
8. Gharpure, P.B.: A cellular automation model of electrical wave propagation in cardiac muscle. Ph.D. thesis, Department of Bioengineering, University of Utah (1996)
9. Luo, C.H., Rudy, Y.: A dynamic model of the cardiac ventricular action potential. II. Afterdepolarizations, triggered activity, and potentiation. Circ. Res. **74**(6), 1097–1113 (1994)
10. MacCannell, K.A., Bazzazi, H., Chilton, L., Shibukawa, Y., Clark, R.B., Giles, W.R.: A mathematical model of electrotonic interactions between ventricular myocytes and fibroblasts. Biophys. J. **92**(11), 4121–4132 (2007)
11. de Oliveira, B.L., Rocha, B.M.R.B.M., Barra, L.P.S., Toledo, E.M., Sundnes, J., dos Santos, R.W.: Effects of deformation on transmural dispersion of repolarization using in silico models of human left ventricular wedge. Int. J. For Numer. Methods Biomed. Eng. 29, 1323–1337 (2013)
12. Rudy, Y.: Electrotonic cell-cell interactions in cardiac tissue: effects on action potential propagation and repolarization. Ann. N. Y. Acad. Sci. **1047**(1), 308–313 (2005)
13. Sampson, K.J., Henriquez, C.S.: Electrotonic influences on action potential duration dispersion in small hearts: a simulation study. Am. J. Physiol. (Heart Circ. Physiol.) **289**, 350–360 (2005)
14. dos Santos, R.W., Plank, G., Bauer, S., Vigmond, E.J.: Parallel multigrid preconditioner for the cardiac bidomain model. IEEE Trans. Biomed. Eng. **51**(11), 1960–1968 (2004)
15. Taggart, P., Sutton, P., Opthof, T., Coronel, R., Kallis, P.: Electrotonic cancellation of transmural electrical gradients in the left ventricle in man. Prog. Biophys. Mol. Biol. **82**(1), 243–254 (2003)

16. Toyoshima, H., Burgess, M.J.: Electrotonic interaction during canine ventricular repolarization. Circ. Res. **43**, 348–356 (1978)
17. Vigmond, E., Dos Santos, R.W., Prassl, A., Deo, M., Plank, G.: Solvers for the cardiac bidomain equations. Prog. Biophys. Mol. Biol. **96**(1–3), 3–18 (2008)
18. Viswanathan, P.C., Shaw, R.M., Rudy, Y.: Effects of i_{Kr} and i_{Ks} heterogeneity on action potential duration and its rate dependence: a simulation study. Circulation **99**(18), 2466–2474 (1999)